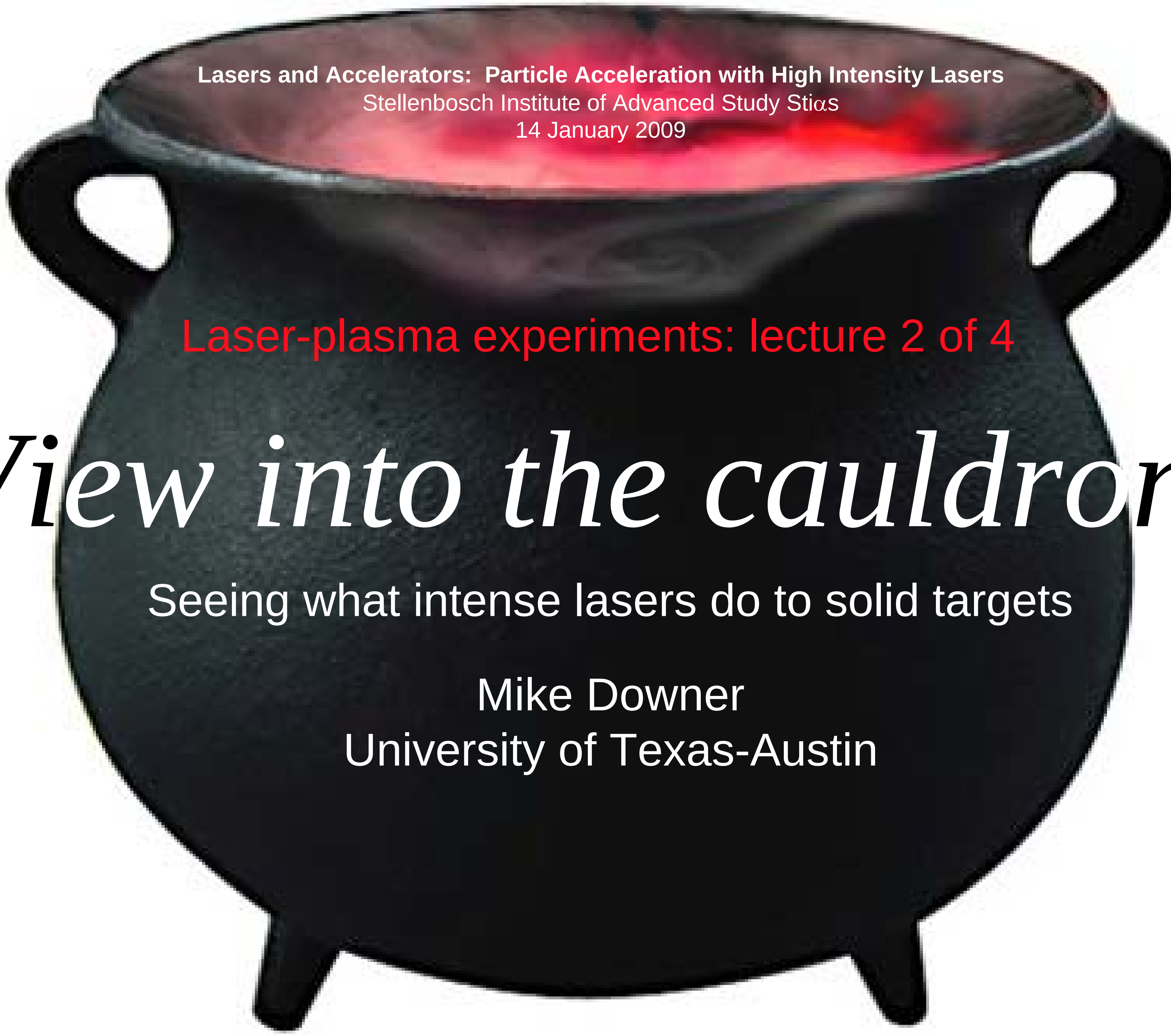

Lasers and Accelerators: Particle Acceleration with High Intensity Lasers

Stellenbosch Institute of Advanced Study Stiαs

14 January 2009

Laser-plasma experiments: lecture 2 of 4

View into the cauldron

Seeing what intense lasers do to solid targets

Mike Downer

University of Texas-Austin

Targets heated by fs pulses are inertially confined...

Picosecond Pulse

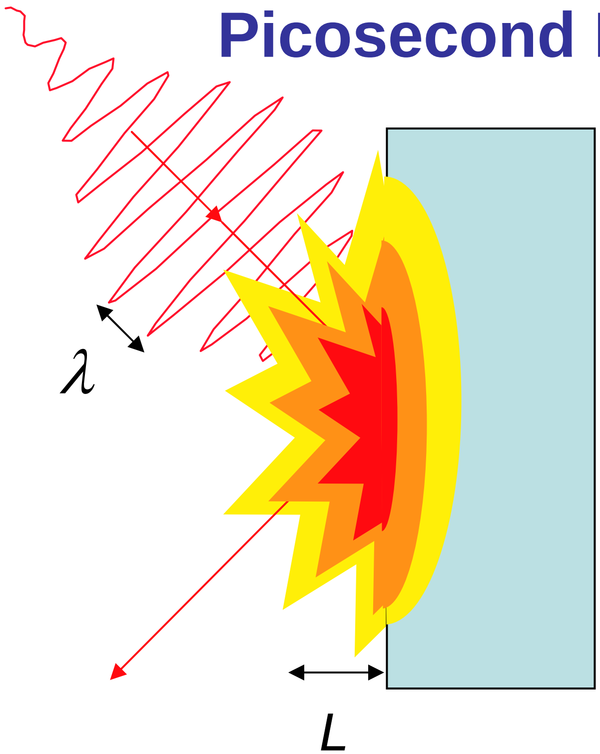

Femtosecond Pulse

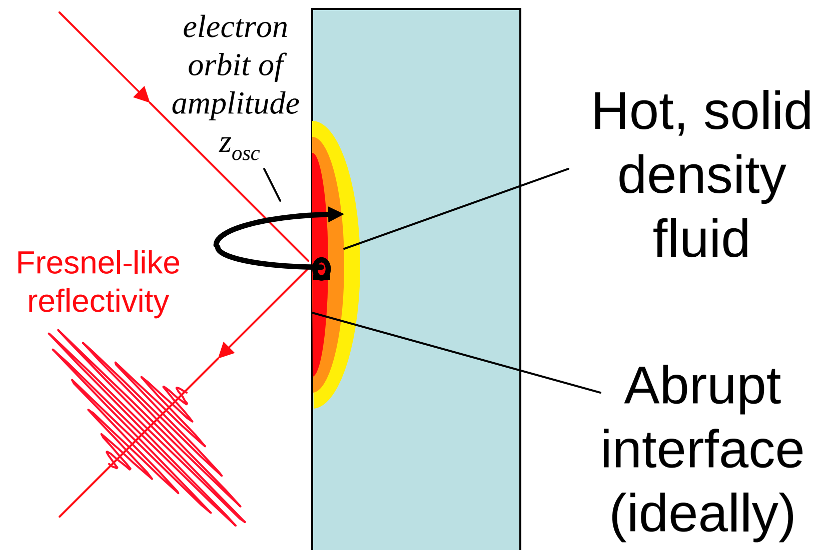

Recent experiments use ultrafast **x-ray**[1] & **proton**[2] irradiation to achieve more <u>uniform</u> isochoric heating than fs optical pulses

[1]Dyer, *J. Mod. Opt.* **50**, 2495 (2003)
[2]____, *Phys. Rev. Lett.* **101**, 015002 (2008)

Interplay among collisional, resonance & vacuum heating absorption governed by relative values of L, λ, and z_{osc}

... and isochorically* heated...

Remington, “Modeling Astrophysical Phenomena in the Laboratory with Intense Lasers,” *Science* **284**, 1488 (1999)

* constant density

brown dwarfs “astrophysical” states of matter

Jupiter interior

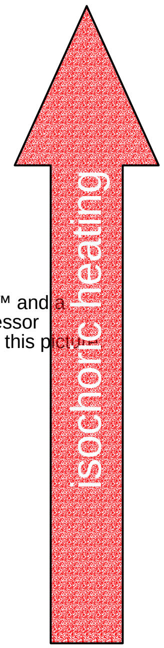

QuickTime™ and a
decompressor
are needed to see this picture.

Warm Dense Matter:
at the crossroads of
condensed matter
& plasma physics

Strongly coupled plasma:

$\Gamma = Z^2e^2/r_0kT_e < 1$

where $r_0 \equiv$ average interatomic spacing

... providing access to exotic states of matter of astrophysical interest

Pump-and-probe experiments measure time evolution of the hot target surface

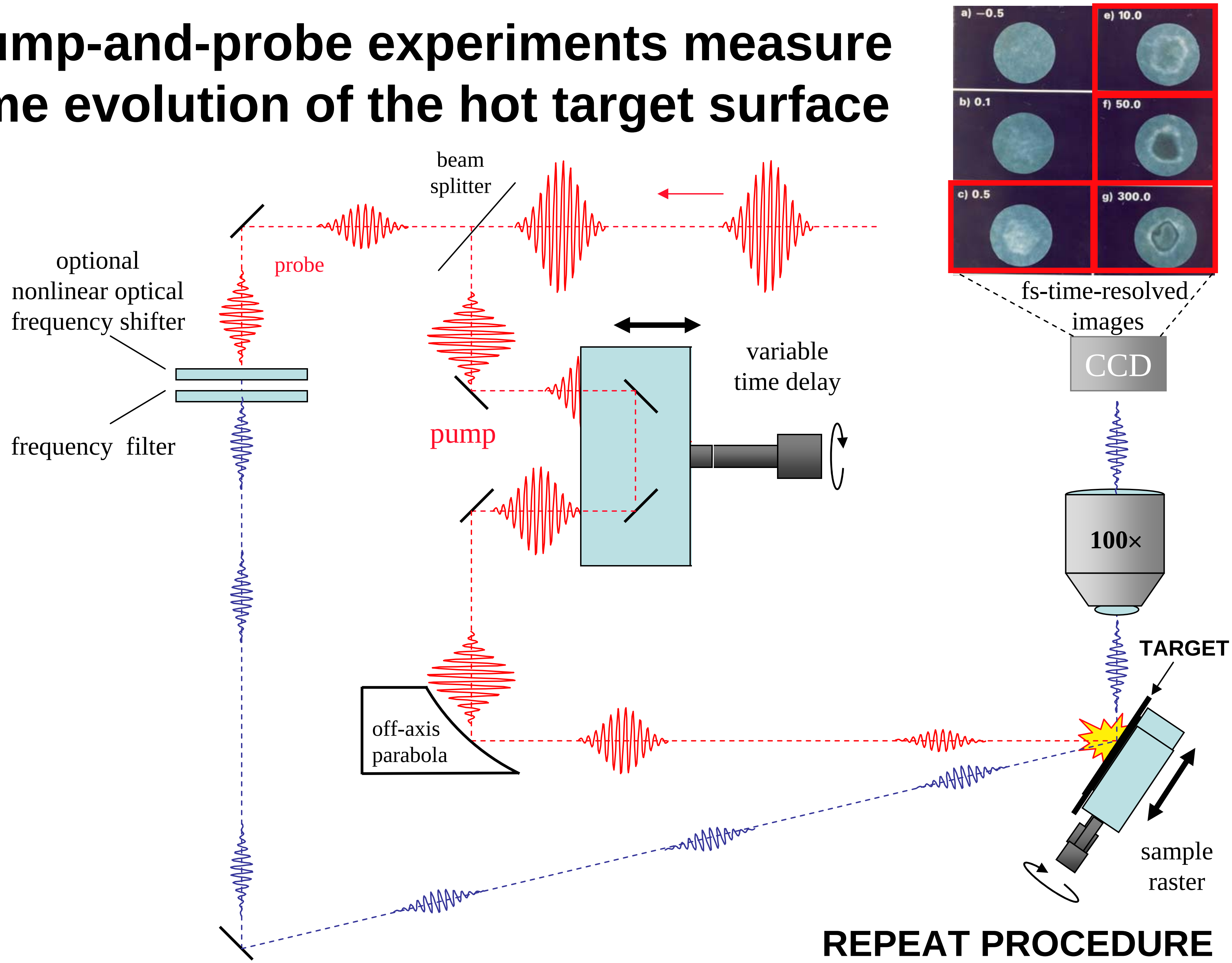

REPEAT PROCEDURE

Femtosecond Movie of Silicon Melting & Evaporation

MD, J. Opt. Soc. Am. B **2**, 595 (1985)

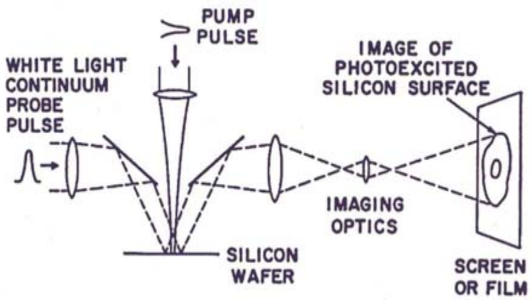

MAJOR EVENTS:

- $\Delta t < 0$: semiconducting Si surface (R = 0.3)
- $-0.04 < \Delta t < 0.04$ ps: pump absorbed
- $\Delta t \approx 1$ ps: liquid metal Si surface (R = 0.6)
- $\Delta t \geq 10$ ps: absorption from ejecta ($R \rightarrow 0$)

Red numbers denote pump-probe time delay Δt in ps

pump parameters:

λ = 620 nm
w_0 = 75 µm on target
τ = 80 fs
energy = 0.1 mJ
E_{max} = 0.5 J/cm^2 on target
I_{max} = 10^{13} W/cm^2 on target

QuickTime™ and a
mpeg4 decompressor
are needed to see this picture.

Silicon melting threshold:

$E_{THRESHOLD}$ = 0.1 J/cm^2

Laboratory observations of solid targets irradiated by intense ultrashort laser pulses

I. Absorption

- resonance
- vacuum heating
- j X B

II. "Hot" electrons

III. X-rays

IV. Magnetostatic Fields

V. Ions

Measurements of fs Resonance Absorption

Single pulse reflectivity

Fedosejevs, *Phys. Rev. Lett.* **64**, 1250 (1990)

τ_p = 250 fs, λ = 248 nm

integrating sphere measured non-specular scatter

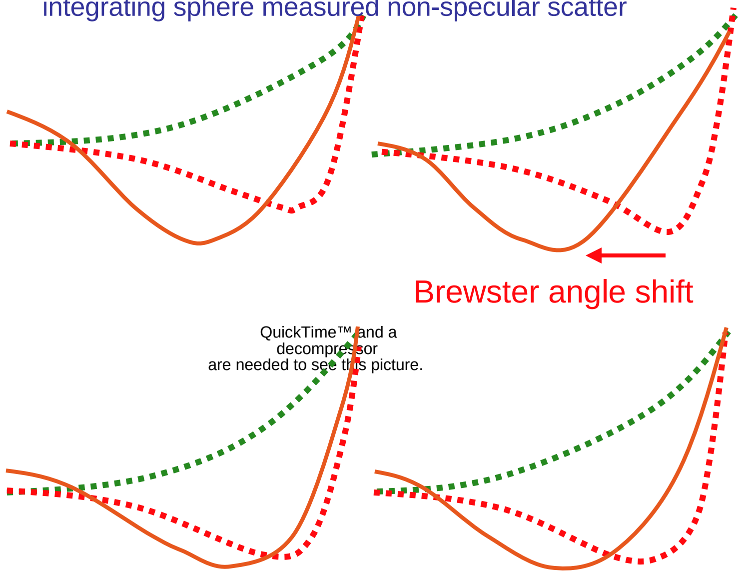

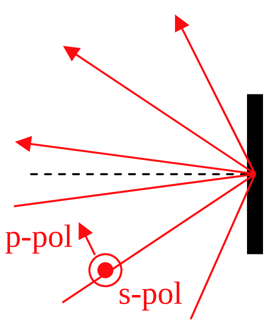

"s" : **E** ⊥ plane of incidence

"p" : **E** || plane of incidence

step $n_e(z)$

(Fresnel-Drude model)

exponential $n_e(z)$

linear $n_e(z)$

(RA model)

Fs time-resolved reflectivity

Wang, *Opt. Lett.* **17**, 1450 (1992)

τ_p = 90 fs, λ = 620 nm, I_{pump} = 10^{13} W/cm^2

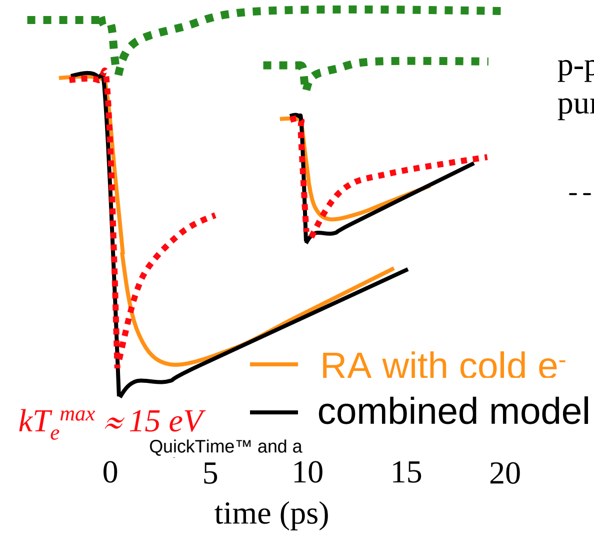

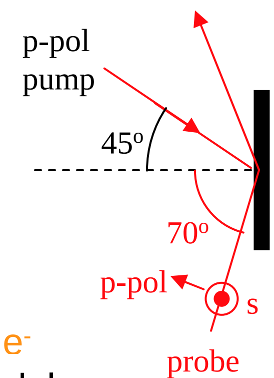

step $n_e(z)$ (Fresnel reflectivity)

$$\varepsilon(t) = 1 - \frac{\omega_p^2}{\omega\ [\omega + \imath\nu(t)]}$$ (Drude dielectric function for free-electron metals)

$$\nu(t) = C n_i Z^2 T_e(t) / \omega_p^2$$ (electron-ion collision frequency for kT_e < 20 eV)

$$C_e(T_e)\frac{\partial T_e}{\partial t} = K\nabla^2 T_e - g(T_e - T_i) + \underbrace{A(r,t)}_{\text{pump absorption}}$$

$$C_i\frac{\partial T_i}{\partial t} = g(T_e - T_i)$$

collisional electron heating & cooling model

heat capacities — *electron-phonon coupling coefficient*

Surface expansion also shifts phase $\Delta\phi_{s,p}$ of probe pulse; <u>frequency-domain-interferometry</u> (FDI) measures this shift

Froehly, *J. Opt. (Paris)* **4**, 183 (1973); Blanc, *J. Opt. Soc. Am. B* **13**, 118 (1996)

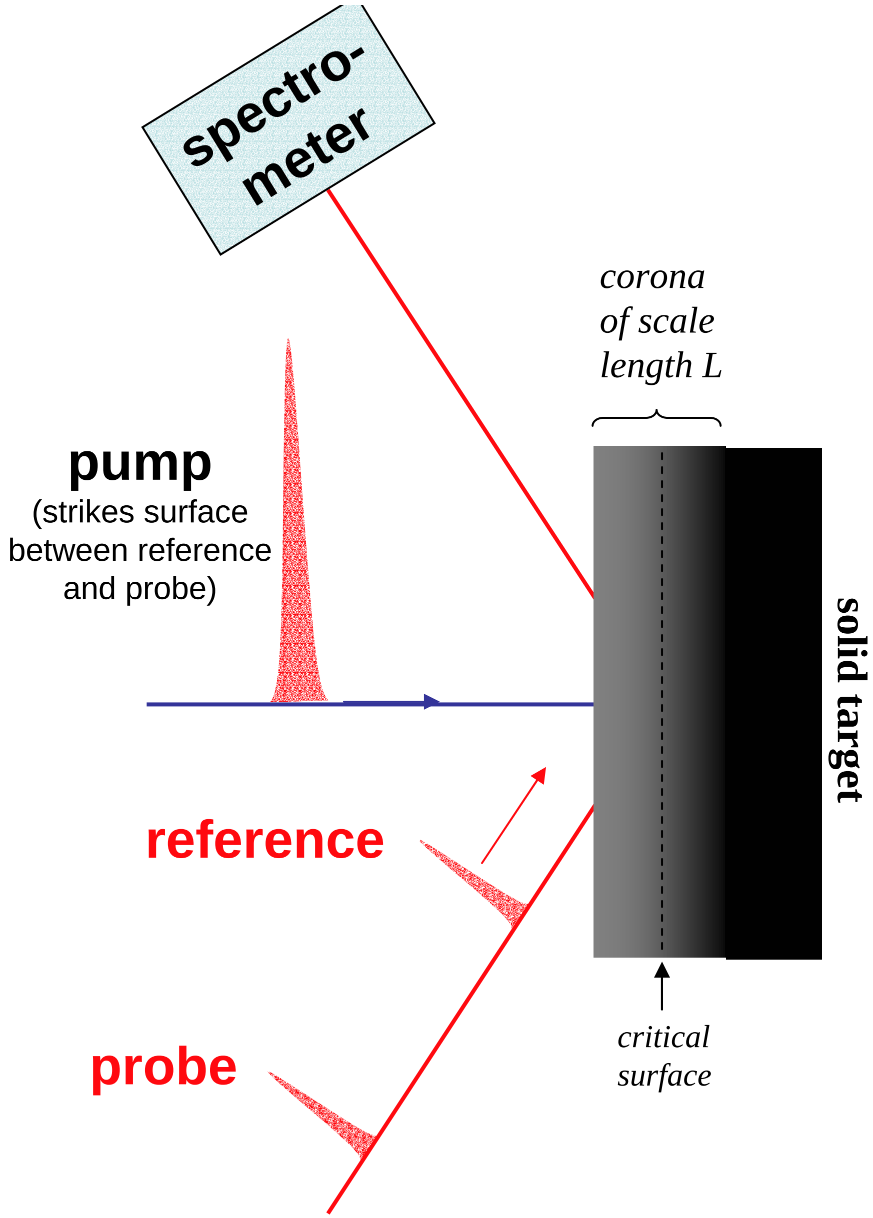

τ_p = 100 fs, λ = 620 nm, $I_{pump} \approx 10^{15}$ W/cm^2, θ_{probe} = 60^o

Fe target

probe phase shift

probe reflectivity

and a
decompressor
are needed to see this picture.

data from Grimes *et al*., *Phys. Rev. Lett*. **82**, 4010 (1999)

Surface expansion also shifts phase $\Delta\phi_{s,p}$ of probe pulse; frequency-domain-interferometry (FDI) measures this shift

Froehly, *J. Opt. (Paris)* **4**, 183 (1973); Blanc, *J. Opt. Soc. Am. B* **13**, 118 (1996)

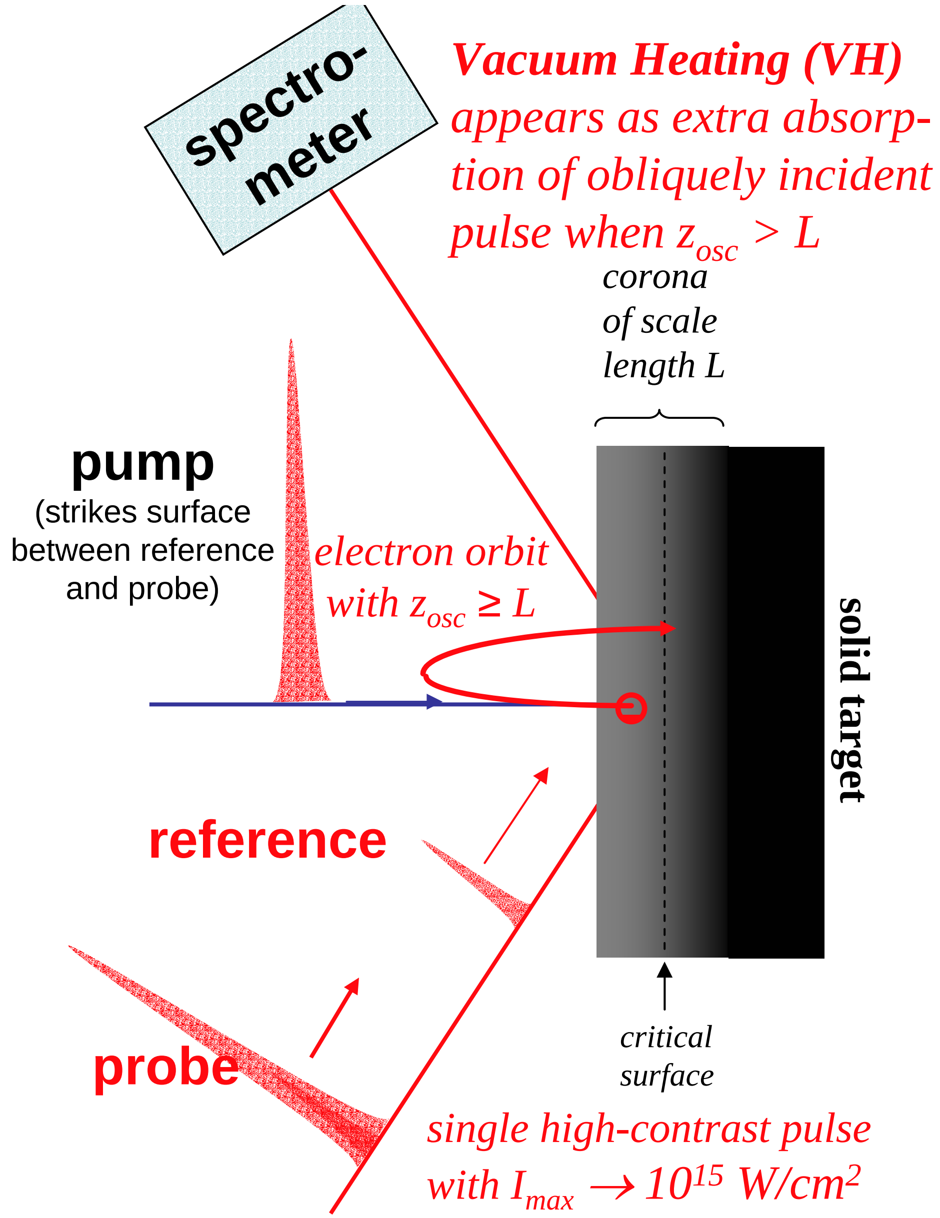

τ_p = 100 fs, λ = 620 nm, $I_{pump} \approx 10^{15}$ W/cm^2, $\theta_{probe} = 60^o$
peak-to-pedestal contrast: >10^5 @ 1 ps; >10^3 @ 0.2 ps

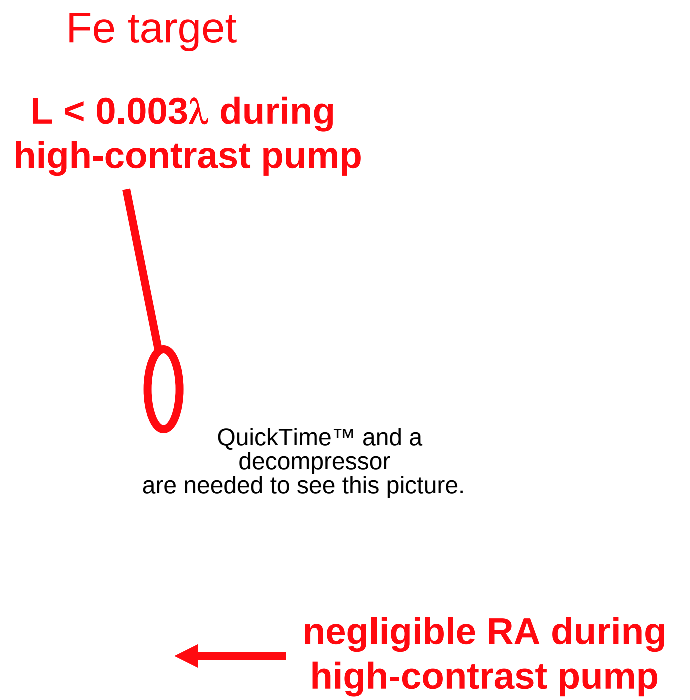

data from Grimes *et al*., *Phys. Rev. Lett*. **82**, 4010 (1999)

“Extra” absorption of intense, high-contrast, obliquely-incident, p-pol pulse when $z_{osc} \geq L$ reveals Vacuum Heating

Grimes *et al.*, *Phys. Rev. Lett.* **82**, 4010 (1999)
Chen, *Phys. Plasmas* **8**, 2925 (2001)

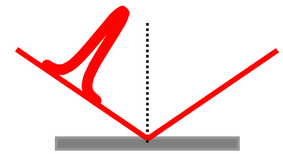

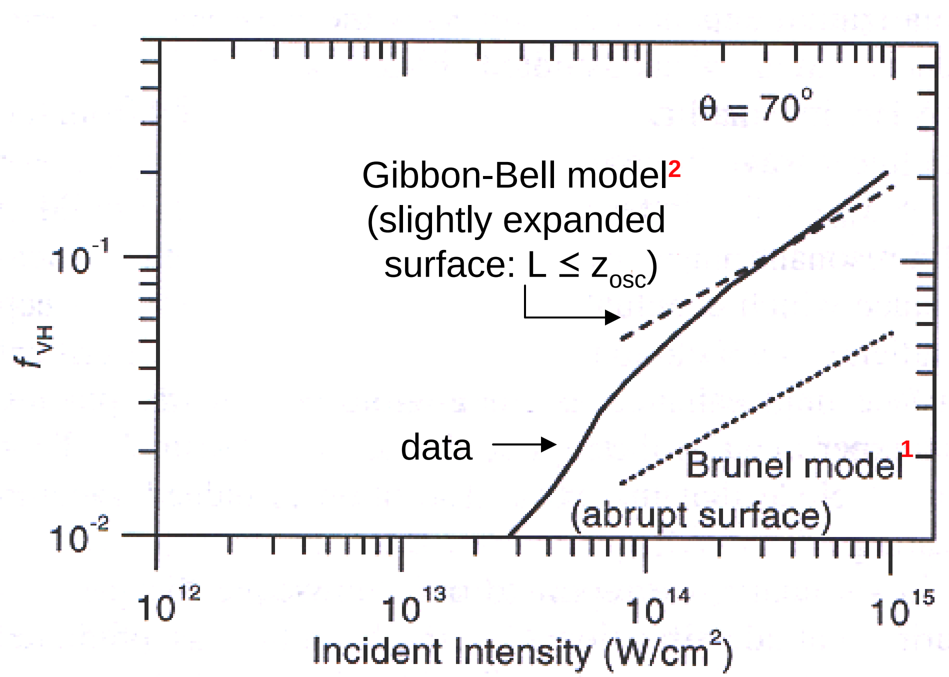

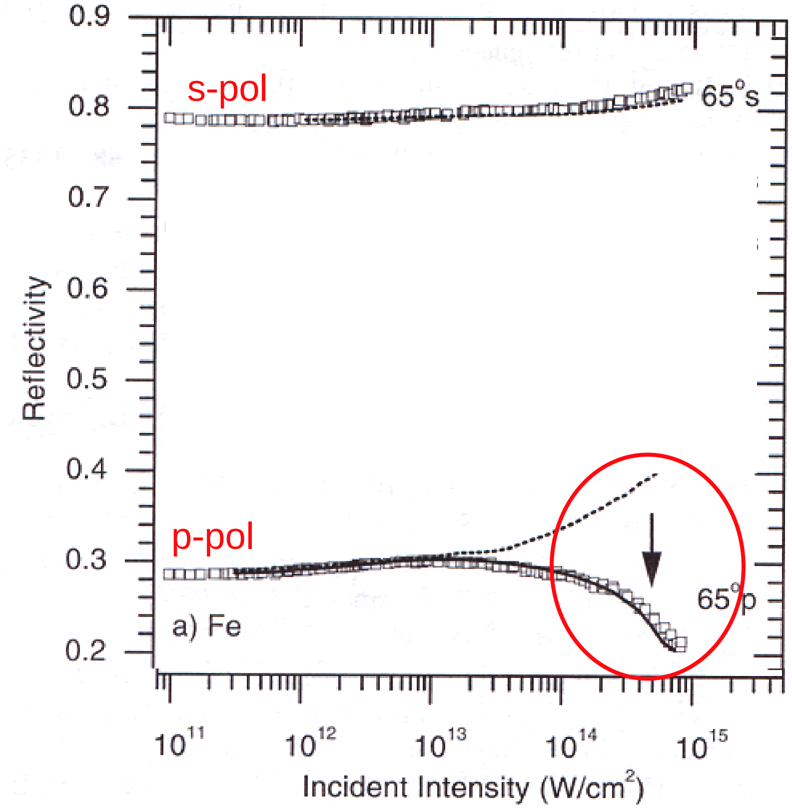

[1] Brunel, *Phys. Rev. Lett.* **59**, 52 (1987)
[2] Gibbon & Bell, *Phys. Rev. Lett.* **68**, 1535 (1992)

Magnitude of VH absorption agrees with first principles models

Extra VH absorption is ...

... strongest for large θ_{inc} (as expected)

... independent of target material (as expected)

II. “Hot” electrons

Simulation of hot electrons produced by RA

Kruer, *The Physics of Laser Plasma Interactions* (Addison-Wesley 1988), c. 10

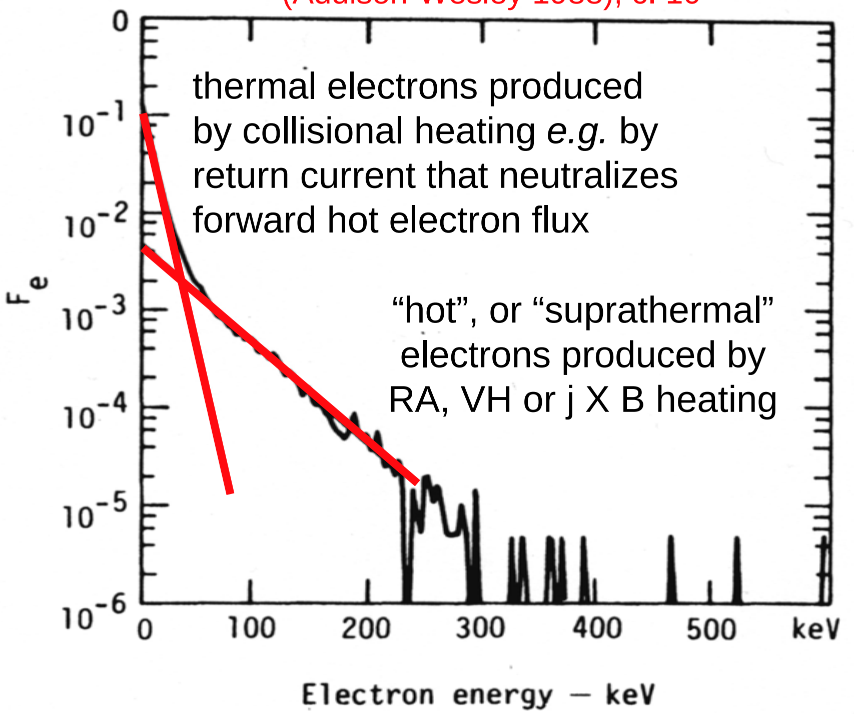

Measured hot electron energy distribution from 50 μm Al foil irradiated at ~10^{18} W/cm^2 by 0.6 ps laser pulse

Zheng, *Phys. Rev. Lett.* **92**, 165001 (2004)

QuickTime™ and a decompressor are needed to see this picture.

A universally observed and calculated feature of intense laser-solid target interactions is production of two electron temperatures

An electron crossing a dielectric interface emits Optical Transition Radiation (OTR)

Ginzburg and Frank, JETP **16**, 15 (1946)
Jackson, *Classical Electrodynamics*, 3rd ed., Sec. 13.7

A single electron emits a broad OTR spectrum

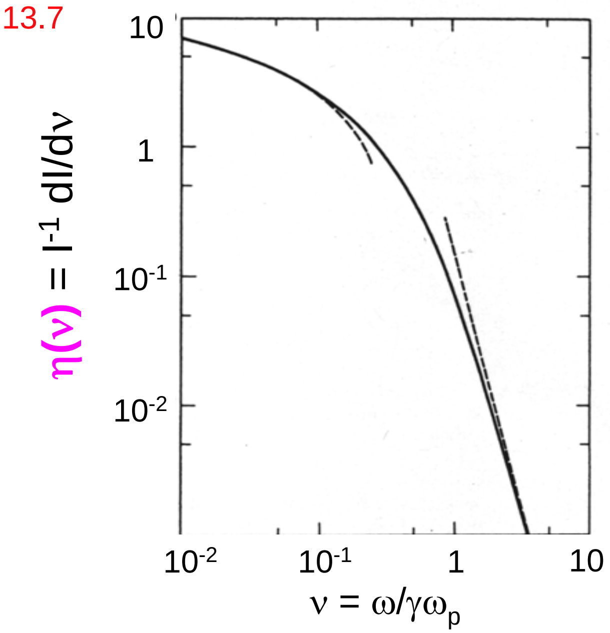

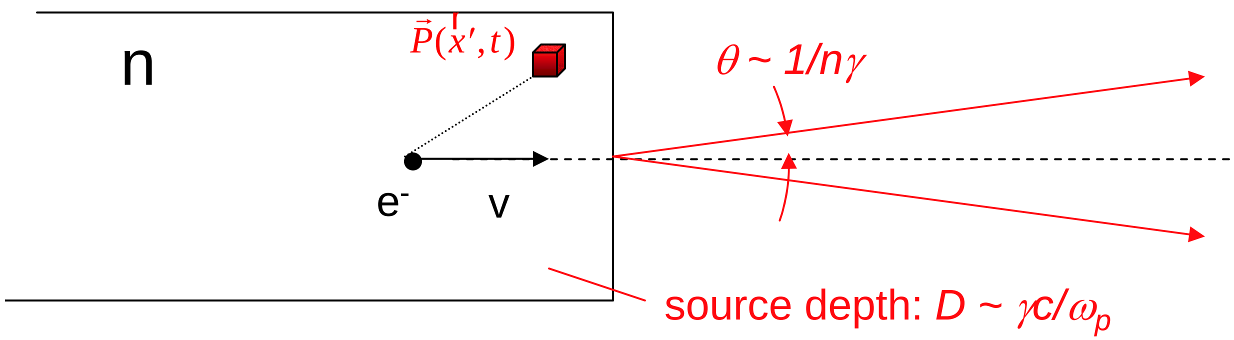

Transition Radiation
(where fields from moving e^- and induced polarization $\vec{P}(\vec{x}',t)$ interfere constructively)

$\gamma \equiv [1 - v^2/c^2]^{-1/2}$

OTR has become a powerful tool for characterizing hot electrons generated by intense laser-plasma interactions

RA, VH & jxB absorption create micro-bunched hot electrons, which emit Coherent Transition Radiation (CTR)

Shibata, *Phys. Rev. E* **50**, 1479 (1994); Zheng, *Phys. Plasmas* **10**, 2994 (2003)

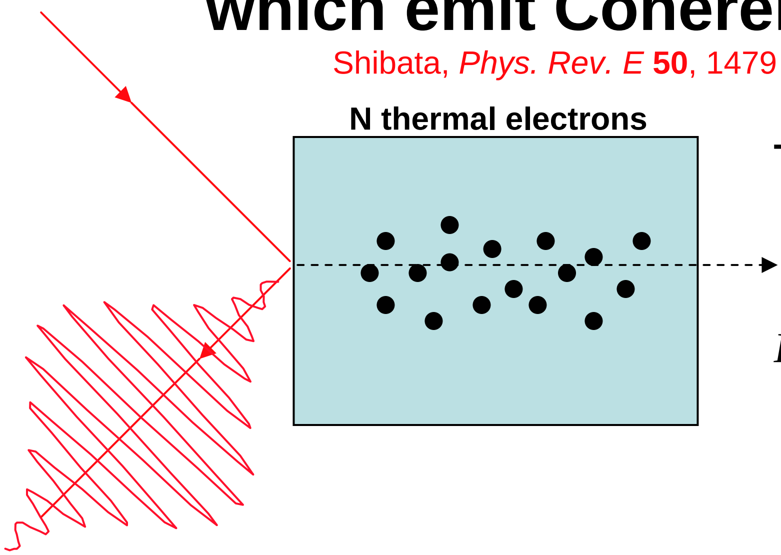

TR from individual electrons adds incoherently:

$$I_{TR}(\nu) = N\underbrace{\eta(\nu)}_{\text{single } e^- \text{ TR spectrum}}$$

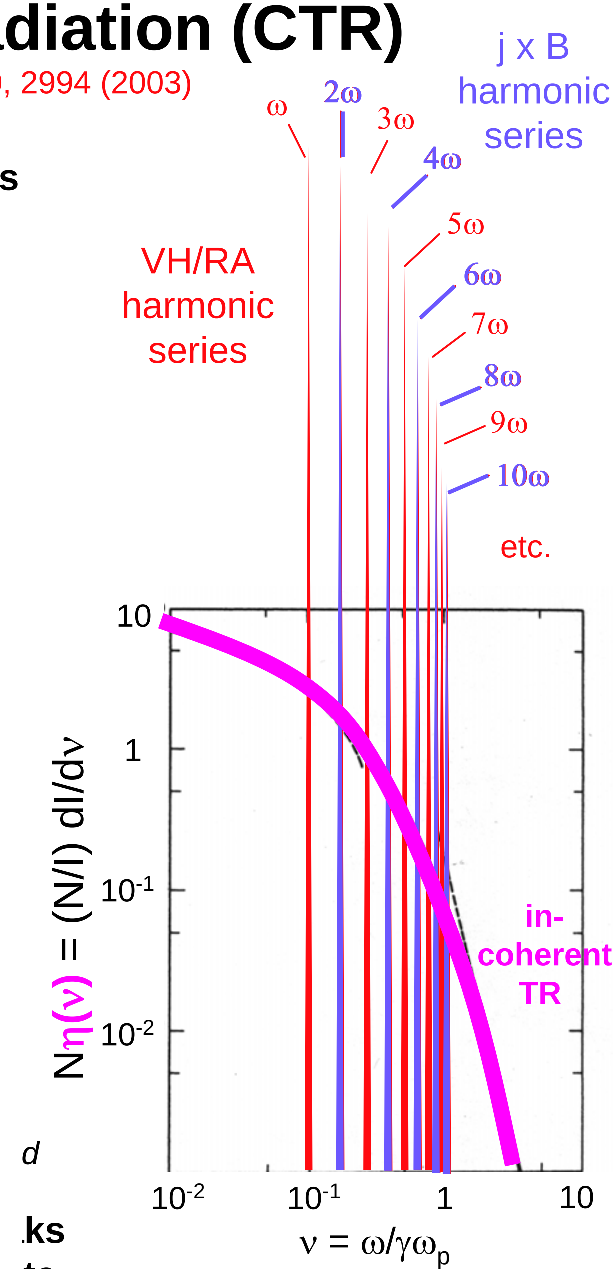

Observations of CTR at $2\omega_{laser}$ demonstrate microbunching of hot electrons

Baton, *Phys. Rev. Lett*. **91**, 105001 (2003); Santos, *Phys. Plasmas* **14**, 103107 (2007)

Blackbody radiation at **kT_e ~ 0.5 MeV** observed on ns time scale, due to resistive target heating by return current neutralizing forward fast e- flux. **These electrons contain ~35% of the incident laser energy.**

QuickTime™ and a decompressor are needed to see this picture.

normally incident laser

spectrum & time evolution of CTR

Decay of CTR signal with increasing target thickness enables an estimate of hot electron temperature

broad incoherent OTR

prompt CTR...

QuickTime™ and a decompressor are needed to see this picture.

QuickTime™ and a decompressor are needed to see this picture.

incoherent OTR

The micro-bunched electrons responsible for CTR contain < 1% of the incident laser energy.

... sharply peaked around $2\omega_{laser}$

CTR observations at $2\omega_{laser}$ with obliquely-incident laser reveal TWO hot electron streams

Cho, *Phys. Plasmas*, in press (2009)

Laser: I = 2 x 10^{19} W/cm^2, θ = 45°, λ = 800 nm

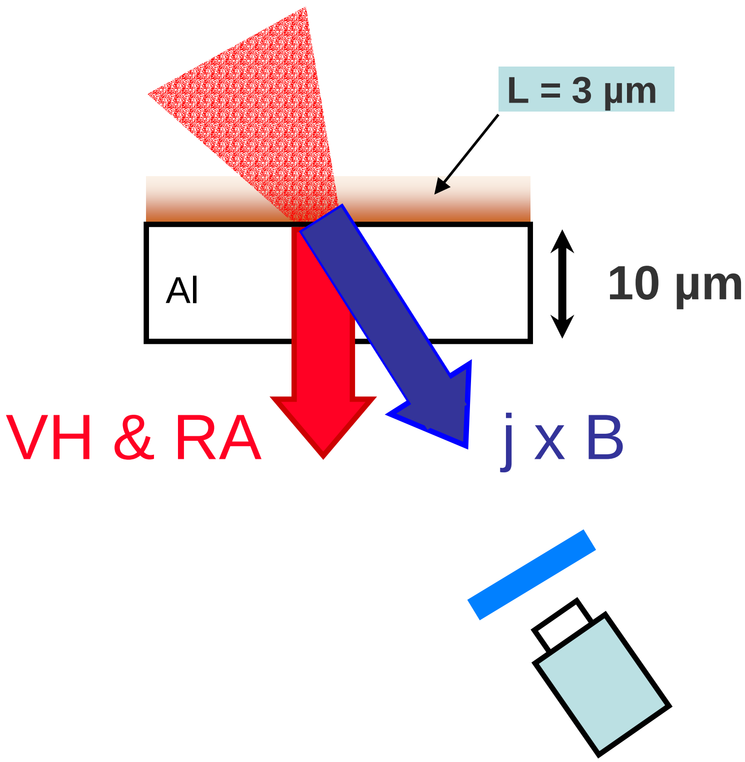

$2\omega_{laser}$ CTR from 10 μm Al foil

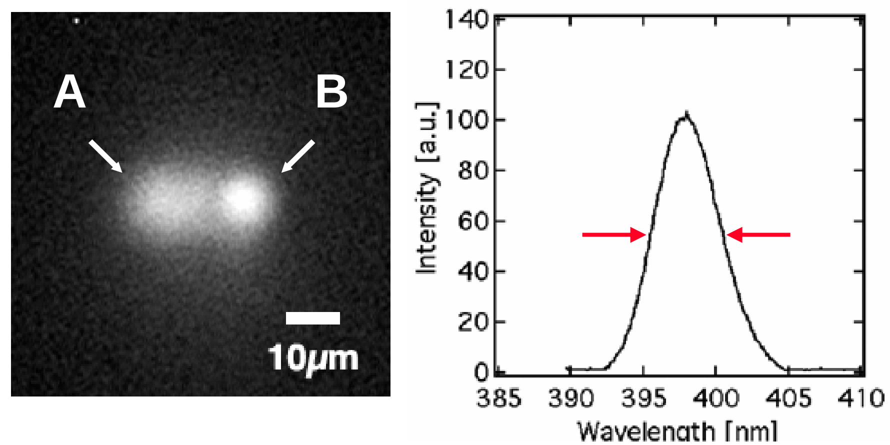

Area of spot A is 3.5x larger than B

This observation clearly distinguishes j x B heating from VH & RA

CTR images reveal self-organized filaments in fast electron beam

Jung, *Phys. Rev. Lett.* **94**, 195001 (2005)

SIMULATION

attributes behavior to Weibel instability

propagation distance

e^- density **magnetic field**

QuickTime™ and a decompressor are needed to see this picture.

10 µm

20 µm

QuickTime™ and a decompressor are needed to see this picture.

QuickTime™ and a decompressor are needed to see this picture.

100 µm

Grazing-incidence laser pulses produce hot e⁻ that skate along the target surface

Li, *Phys. Rev. Lett.* **96**, 165003 (2006)

LASER: 0.6 J, 30 fs, 800 nm, ~10^{18} W/cm^2

TARGET: 30 μm Al foil

Simulations show large quasistatic self-generated B & E fields confine SFEs to oscillating trajectories along target surface

θ = 22°

θ = 45°

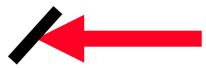

SFE trajectories

QuickTime™ and a decompressor are needed to see this picture.

θ = 70°

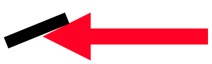

QuickTime™ and a decompressor are needed to see this picture.

⊥ target surface

PROPERTIES OF SURFACE FAST ELECTRONS (SFEs):

$kT_{SFE} \approx$ 0.3 MeV

~ 10^{10} SFEs for θ = 70°

Detected by Image Plate (IP) stacks surrounding laser focus

B_z and $E_\perp$ are normalized to incident laser field $m\omega c/e$

Laser-generated hot electrons ...

- transport 30-40% of intense laser pulse energy into target
- propagate mainly along target normal (VH, RA), incident laser direction (j X B), and target surface
- produce currents of ~ 10^7 A, current densities > 10^{12} A/cm^2

... and are important for:

- **fast ignition of laser fusion**
- **producing ultrafast x-ray pulses for flash radiography**
- **compact acceleration of ions**

Fast ignition of inertial confinement fusion

Tabak, *Phys. Plasmas* **1**, 1626 (1994); Key, *Nature* **412**, 775 (2001)

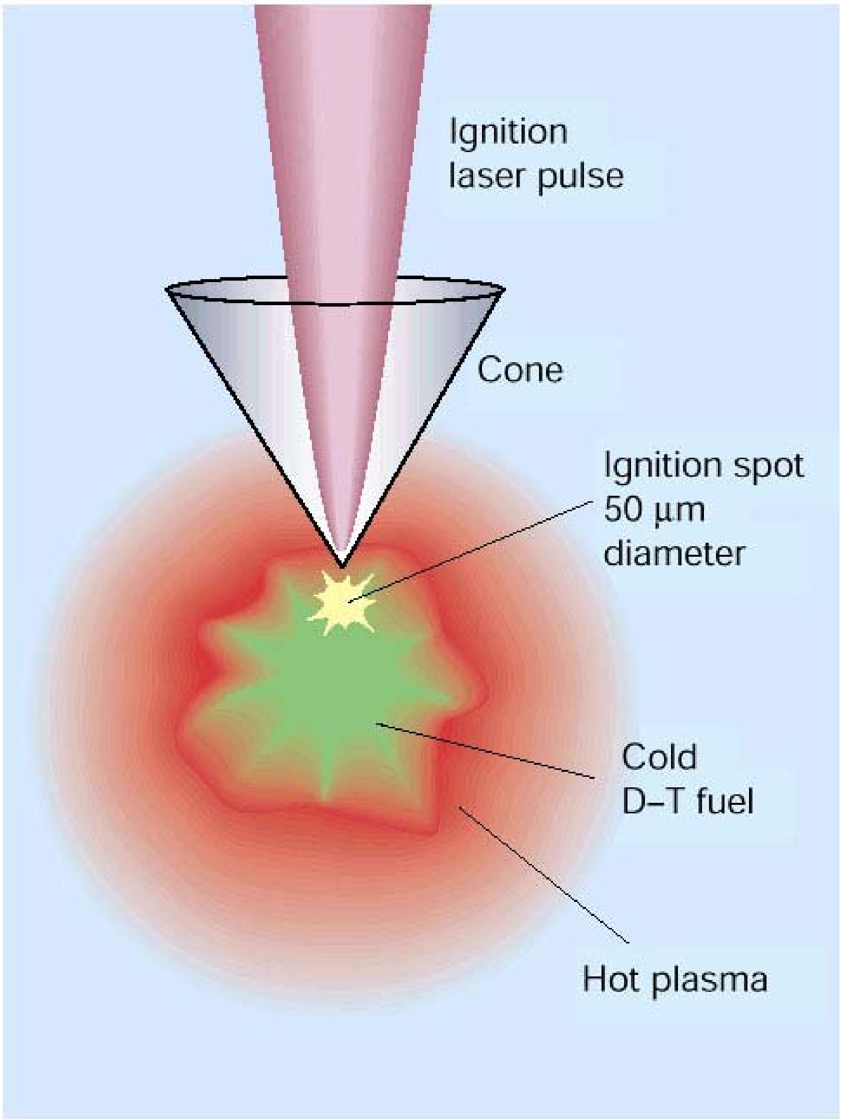

ADVANTAGES OVER CONVENTIONAL ICF:

- separate fuel compression from fuel heating
- reduce fuel density ~5×
- produce fusion energy ~20× more efficiently
- relax stringent requirements on smoothness & sphericity of fuel capsule & uniformity of drive pressure

INITIAL DEMONSTRATIONS EXPLOIT LASER-DRIVEN SFEs TO ENHANCE NEUTRON YIELD

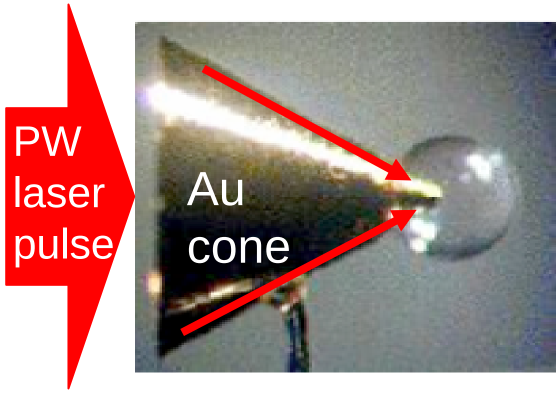

Kodama, *Nature* **412**, 798 (2001); **418**, 933 (2002)

III. X-rays

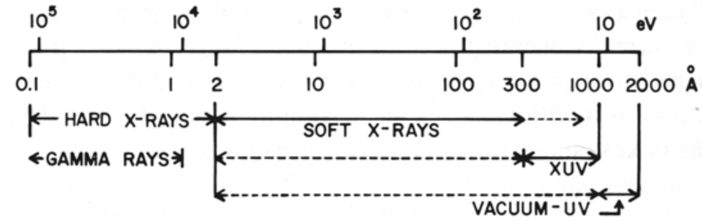

Laser-generated hot electrons produce x-rays by two dominant mechanisms

Kmetec, "MeV X-ray generation with a femtosecond laser," *Phys. Rev. Lett.* **68**, 1527 (1992)
Rousse, "Efficient Kα X-ray source from fs-laser-produced plasmas," *Phys. Rev. E* **50**, 2200 (1994)

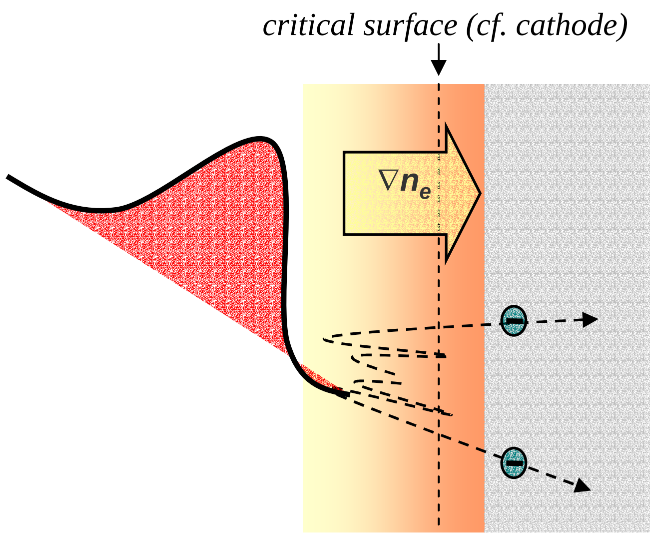

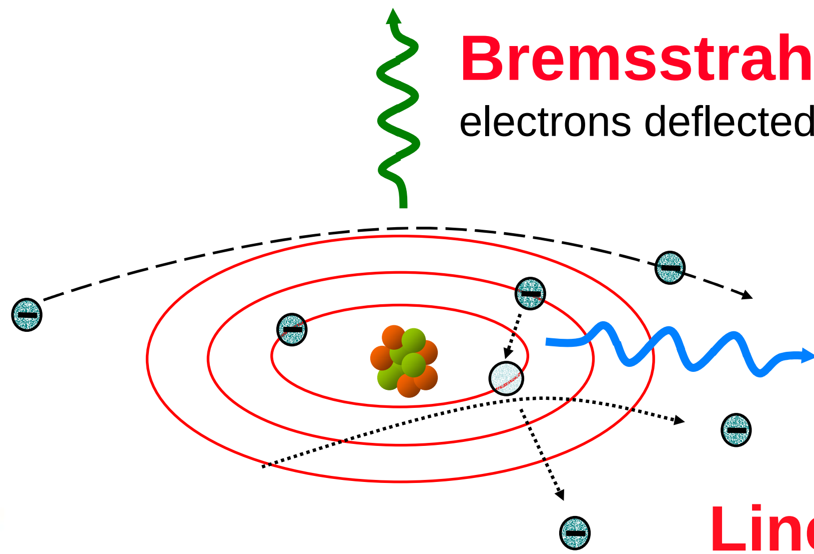

Bremsstrahlung:
electrons deflected by nucleus

Line emission:
Fast electrons knock free core electrons from the inner shell

(typical recombination lifetimes: several fs)

conventional X-ray tube:

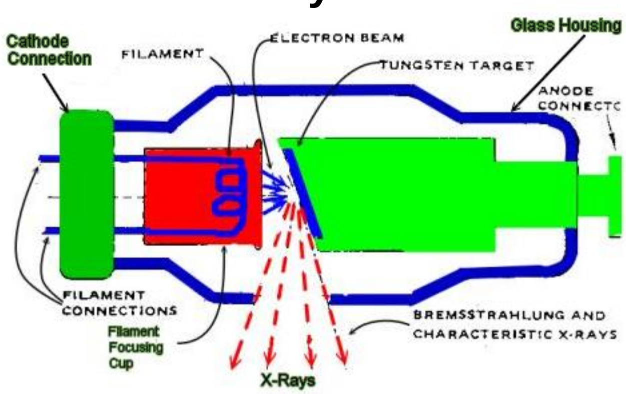

X-ray line spectroscopy is a standard method to infer electron temperature & density in laser-produced plasmas

Basic principles: Griem, *Spectral Line Broadening by Plasmas* (Academic, NY 1974)

Applications to suprathermal electrons: Theobald, *Phys. Plasmas* **13**, 043102 (2006); Koch, *Phys. Rev. E* **65**, 016410 (2001) **[PW lasers]**
Kodama, *Phys. Plasmas* **8**, 2268 (2001); Eder, *Appl. Phys. Lett.* **70**, 211 (2000);
Yasuike, *Rev. Sci. Instrum.* **72**, 1236 (2001); Rousse, *Phys. Rev. E* **50**, 2200 (1994) **[TW lasers]**

Typical experimental setup

Lead shielding

QuickTime™ and a decompressor are needed to see this picture.

Cu foil target

LASER

CCD

X-rays

• When an x-ray photon is absorbed in a pixel, a number of charged carriers proportional to the x-ray photon energy is created (typically one carrier for each 5 eV of photon energy).

• Data from all pixels are collected to compile a single-shot x-ray spectrum.

• Exposure must be limited to << 1 x-ray photon per pixel per shot.

Nishiuchi, *EUV, X-ray, γ-ray Instrumentation for Astronomy IX*, SPIE **3445**, 268 (1998).

K-shell spectrum of Cu target irradiated by 0.7 ps, 447 J laser pulses @ 3×10^{20} Wcm^2

Bremsstahlung continuum subtracted

QuickTime™ and a decompressor are needed to see this picture.

from Theobald (2006)

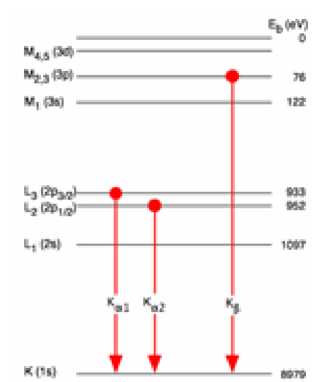

Relative line strengths change with laser intensity and kT_e

QuickTime™ and a decompressor are needed to see this picture.

from Theobald (2006)

Such data contributes to developing scaling laws for e.g.

$$kT_e \text{ vs. } I_{laser}$$

Measurements are time-integrated

Bremsstrahlung continuum x-rays also measure kT_e

Nees, JSTQE **12**, 223 (2006)

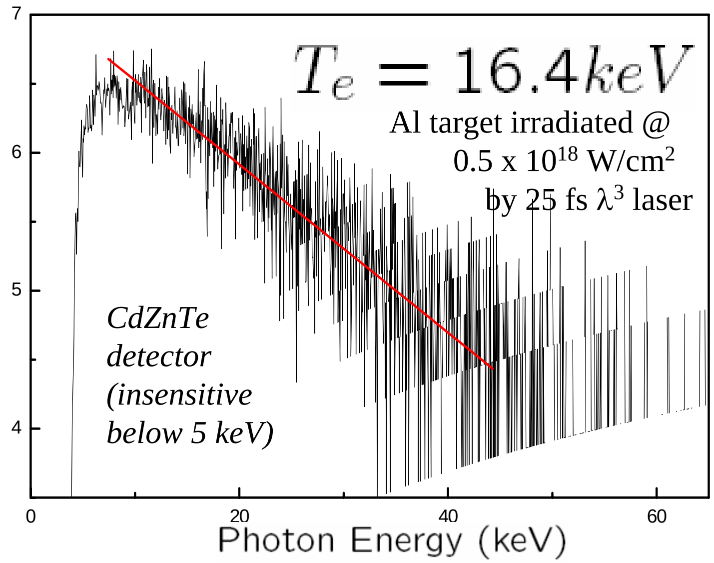

Beg, *Phys. Plasmas* **4**, 447 (1997)

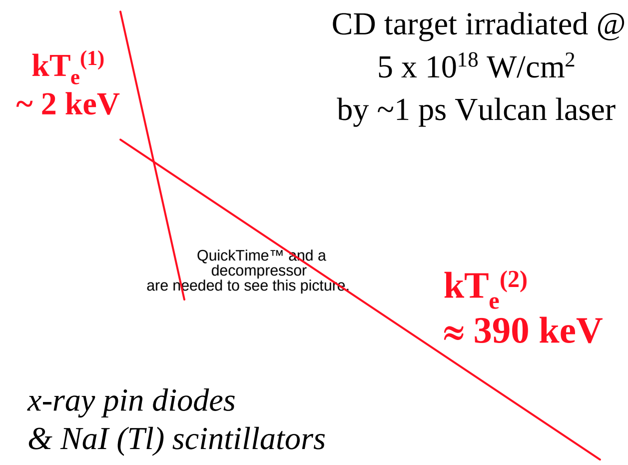

Some studies have correlated X-ray spectroscopy with independent measurements of kT_e based on *e.g.*

- energy spectra of emitted electrons (Zheng, *Phys. Rev. Lett.* **92**, 165001 (2004)) and ions (Tan, *Phys. Fluids* **27**, 296 (1984); Beg, *Phys. Plasmas* **4**, 447 (1997))
- CTR vs. target thickness (Cho, *JOSA B* **25**, B50 (2008); Baton, *Phys. Rev. Lett.* **91**, 105001 (2003))

to yield empirical scaling laws that are widely used:

e.g. $$\boxed{kT_e = 100\,(I_{17}\lambda_{\mu m}^2)^{1/3}\ \text{keV}}$$

Beg, *Phys. Plasmas* **4**, 447 (1997)
for experiments in which RA is
the dominant source of hot electrons

Tightly focused fs lasers create the world's smallest hard x-ray source (~4 μm) for precision imaging

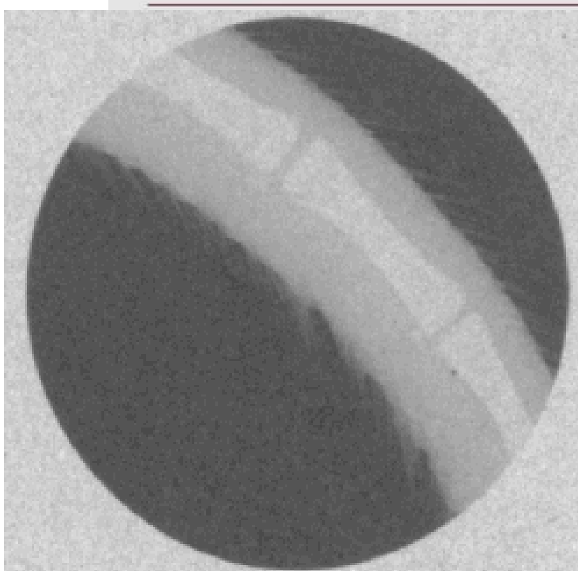

x-ray picture of rat tail: Cu target

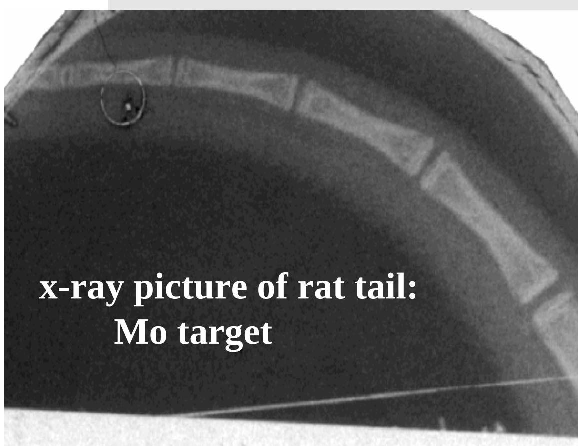

x-ray picture of rat tail:
Mo target

Hou *et al*., *Appl. Phys. Lett*. **84**, 2259 (2004)

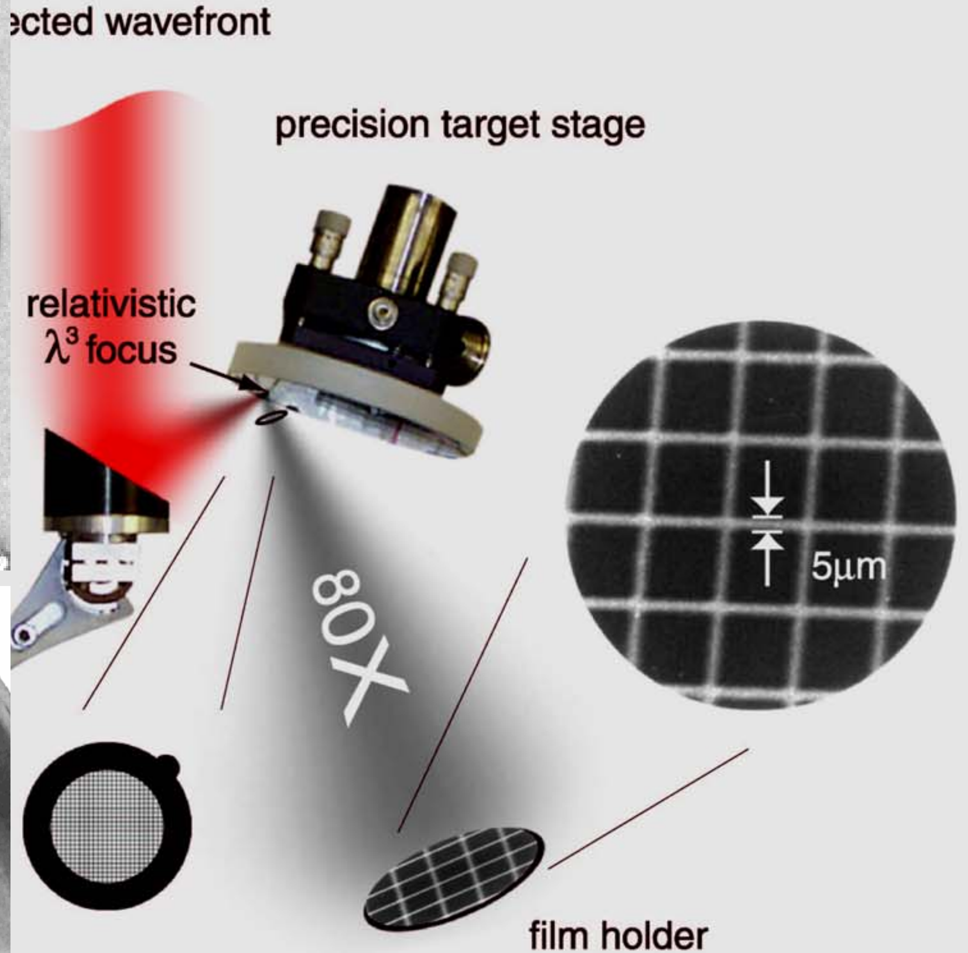

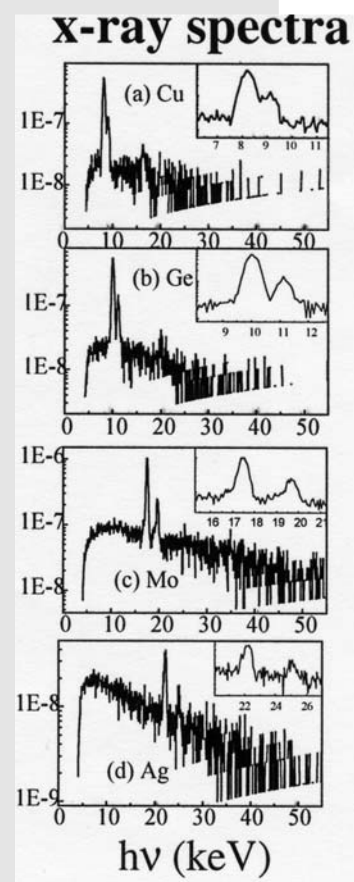

x-ray source size is ~ 4× larger than laser focus
because of lateral heat transport*

*Bowes, *Opt. Lett*. **31**, 116 (2006)

Fs X-ray pulses shorter than a molecular vibrational period probe ultrafast structural dynamics of materials

Pfeifer et al., "Femtosecond x-ray science," *Rep. Prog. Phys*. **69**, 443 (2006).

Most fs x-ray experiments to date have used an x-ray probe produced by laser-solid interaction

x-ray diffraction from melting InSb

Lindenberg, *Science* **308**, 392 (2005)

QuickTime™ and a
decompressor
are needed to see this picture.

QuickTime™ and a
decompressor
are needed to see this picture.

Response times $\tau < 200$ fs are observed, placing an upper limit on the x-ray pulse duration

x-ray diffraction showing lattice vibrations in bismuth

Sokolowski-Tinten *et al*., *Nature* 422, 287 (2003)

probe spectrum

QuickTime™ a
decompress
are needed to see this

QuickTime™ and a
decompressor
are needed to see this picture.

typically
~ 10^{11} K_α photons/s

IV. Magnetic Fields

* Lai, *Astrophys. J.* **491**, 270 (1997)

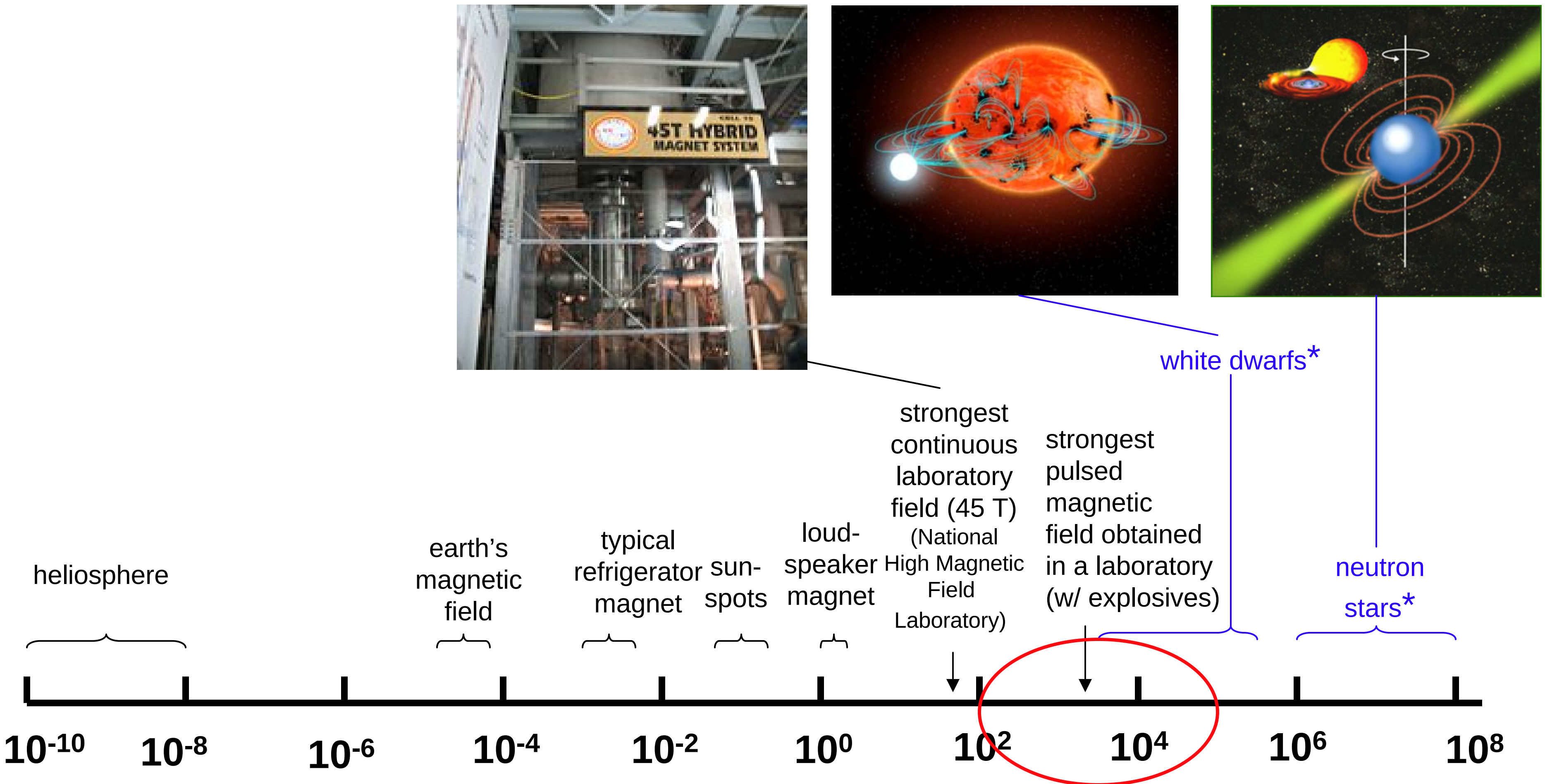

Magnetic Field Strength [Tesla]

Magnetic fields predicted in dense plasmas during relativistic laser-plasma interactions

Wilks, *Phys. Rev. Lett.* **69**, 1383 (1992)
Sudan, *Phys. Rev. Lett.* **70**, 3075 (1993)
Pukhov, *Phys. Rev. Lett.* **76**, 3975 (1996)
Mason, *Phys. Rev. Lett.* **80**, 524 (1998)

Ways to measure them:

- Faraday rotation probe (Stamper, *Phys. Rev. Lett*. **34**, 138 (1975))
- polarimetry of self-generated laser harmonics (Tatarakis, *Nature* (2002))

The strongest B fields produced in relativistic laser-plasma interactions are near the critical surface, where optical harmonics are also generated

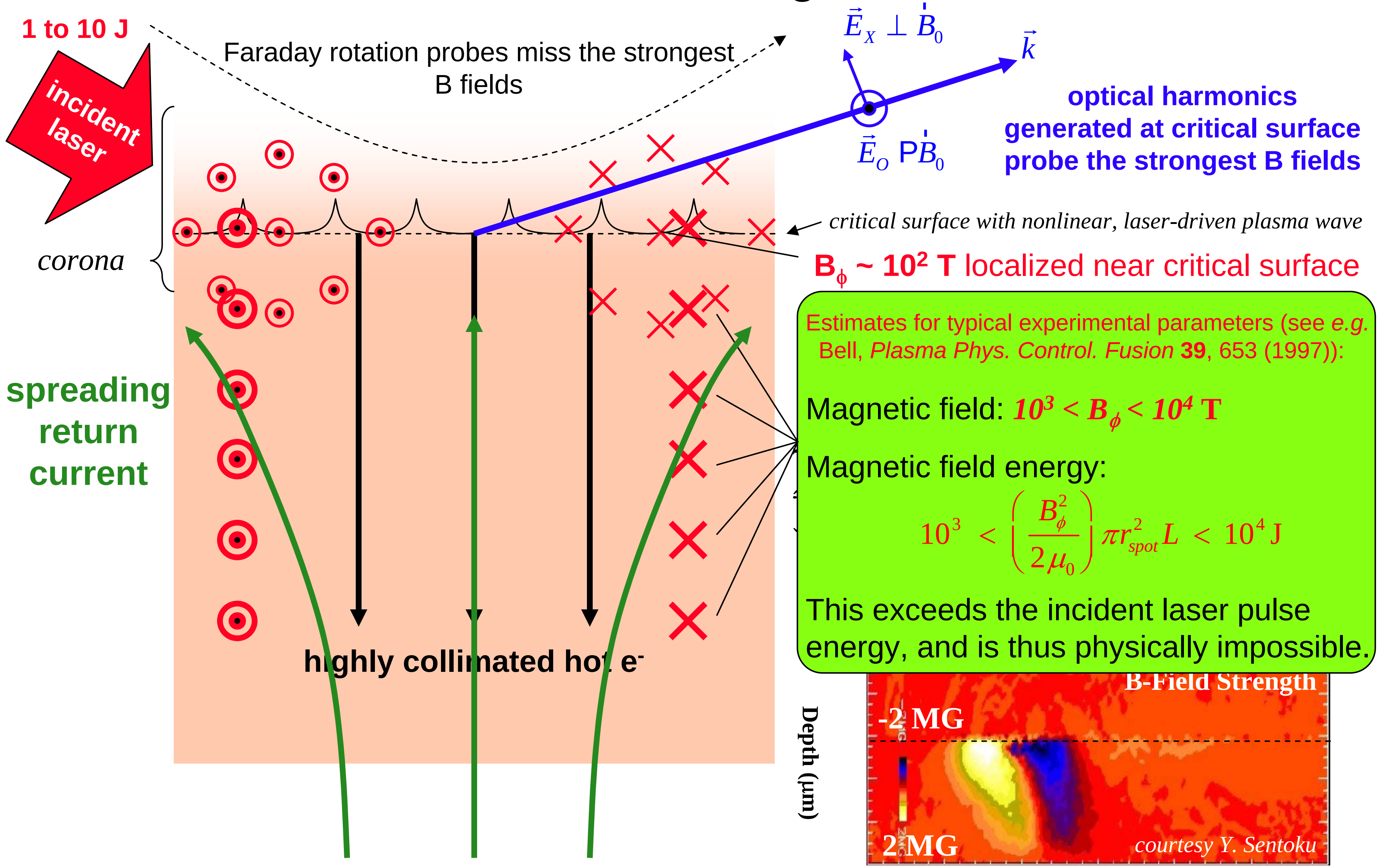

Estimates for typical experimental parameters (see *e.g.* Bell, *Plasma Phys. Control. Fusion* **39**, 653 (1997)):

Magnetic field: $10^3 < B_\phi < 10^4$ T

Magnetic field energy:

$$10^3 < \left(\frac{B_\phi^2}{2\mu_0}\right)\pi r_{spot}^2 L < 10^4 \text{ J}$$

This exceeds the incident laser pulse energy, and is thus physically impossible.

The magnetized plasma is birefringent

Equation of motion of plasma electron: $m\ddot{\vec{x}}(t) = -e\left[\vec{E}_{harm}(t) + \dot{\vec{x}}(t)\times\vec{B}_0\right]$

$$\vec{E}_{harm}(t),\ \vec{x}(t) \propto e^{-i\omega t} \qquad \Rightarrow \qquad \vec{x} = \frac{e}{m\omega^2}\left[\vec{E}_{harm} - i\omega\vec{x}\times\vec{B}_0\right]$$

Obtain dielectric function ε from: $P = -n_e e x \equiv \varepsilon_0\left(\frac{\varepsilon}{\varepsilon_0} - 1\right)E_{harm}$

"Ordinary" or O-wave

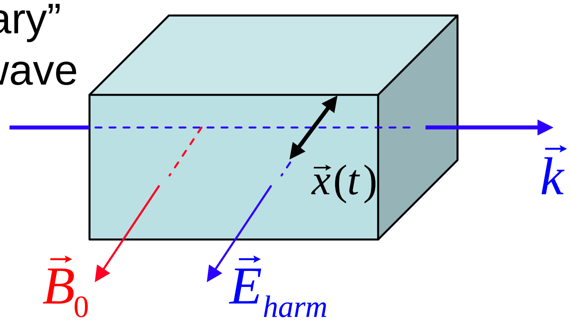

"Extraordinary" or X-wave

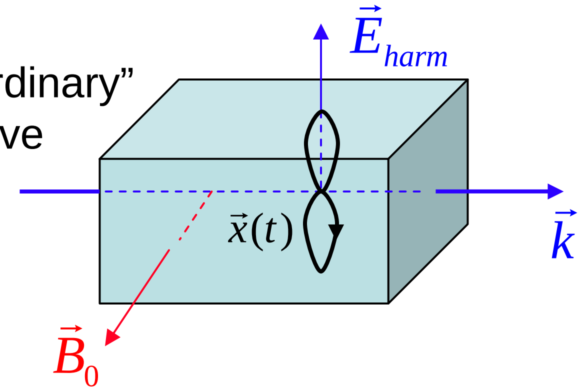

$$\vec{x}\times\vec{B}_0 = 0 \quad \Rightarrow \quad \vec{P} = -\frac{n_e e^2}{m\omega^2}\vec{E}_{harm} = -\varepsilon_0\omega_p^2\vec{E}_{harm}$$

$$\begin{pmatrix} P_x \\ P_y \end{pmatrix} = -n_e e\begin{pmatrix} x \\ y \end{pmatrix} \quad \text{and} \quad \begin{pmatrix} x \\ y \end{pmatrix} = \frac{e^2}{m\omega^2}\begin{pmatrix} E_x - i\omega y B_0 \\ E_y + i\omega x B_0 \end{pmatrix}$$

$$\boxed{\frac{\varepsilon_{/\!/}}{\varepsilon_0} = 1 - \frac{\omega_p^2}{\omega^2}}$$

$$\boxed{\frac{\varepsilon_{\perp}}{\varepsilon_0} = 1 - \frac{\omega_p^2}{\omega^2}\,\frac{\omega^2 - \omega_p^2}{\omega^2 - \omega_h^2}}$$

where $\omega_h^2 = \omega_p^2 - \omega_B^2$

Cutoffs at ω = ω_p
(depend on ω and n_e only)

Cutoffs at $\omega_p^2(\omega^2-\omega_p^2) = \omega^2(\omega^2 - \omega_h^2)$
(depend on ω, n_e and B_0)

Observed harmonic X-wave cutoffs reveal B > 340 T, the strongest B field ever produced in a laboratory

Tatarakis, "Measuring huge magnetic fields," *Nature* **415**, 280 (2002)
Tatarakis, "Measurement of ultrastrong magnetic fields during relativistic laser-plasma interactions," *Phys. Plasmas* **9**, 2244 (2002)

Cutoffs for harmonics:
- 3rd: 220 T
- 4th: 340 T
- 5th: 460 T

at $n_e = 2.4 \times 10^{21}$ cm^{-3}
(relativistically corrected critical density)

QuickTime™ and a decompressor are needed to see this picture.

Vulcan laser parameters:
$\lambda = 1.054$ μm
$\tau_p \sim 1$ ps
Energy ~ 90 J

Plot of X-wave cut-offs for various harmonics

cutoff observed

no cutoff observed

X-wave harmonic emission vs laser intensity

QuickTime™ and a decompressor are needed to see this picture.

no cutoff observed for 5th harmonic

V. MeV Protons & Ion Beams

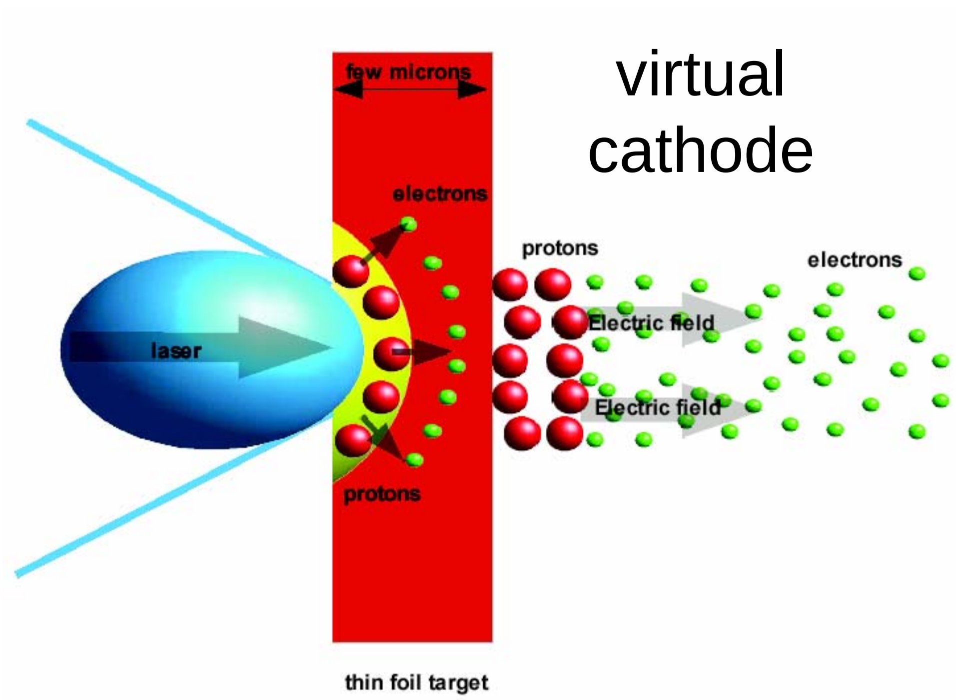

courtesy Prof. Dr. Oswald Willi, U. Düselldorf

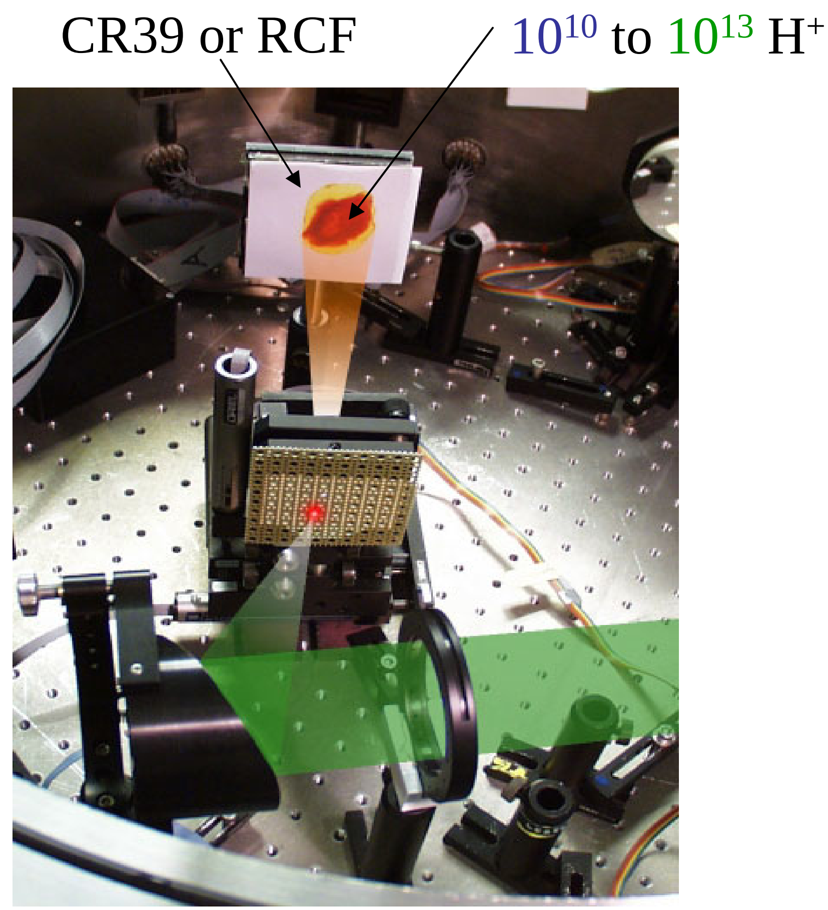

courtesy Prof. Don Umstadter, U. Nebraska-Lincoln

Target Normal Sheath Acceleration: hot electrons traversing target electrostatically accelerate impurity hydrogen ions on the rear surface

Proton Therapy enables precise exposure of small tumors with minimal damage to surrounding healthy tissue ...

... but requires large, expensive facilities

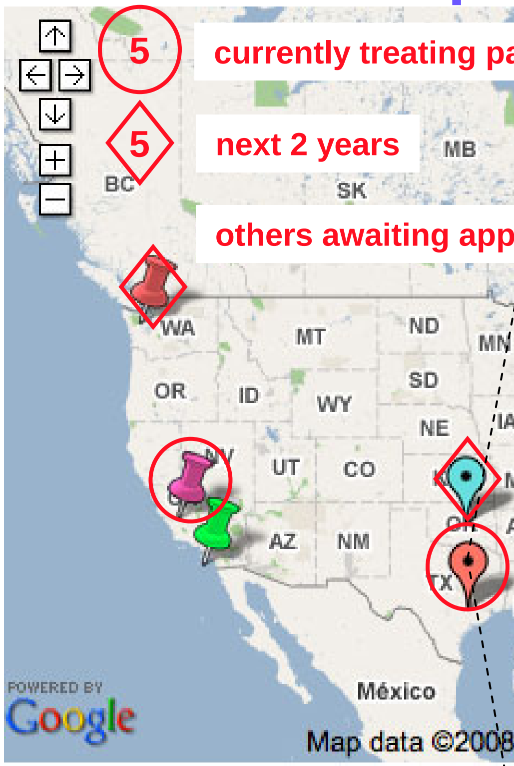

10,000 m^2, \$125 M facility opened in 2006

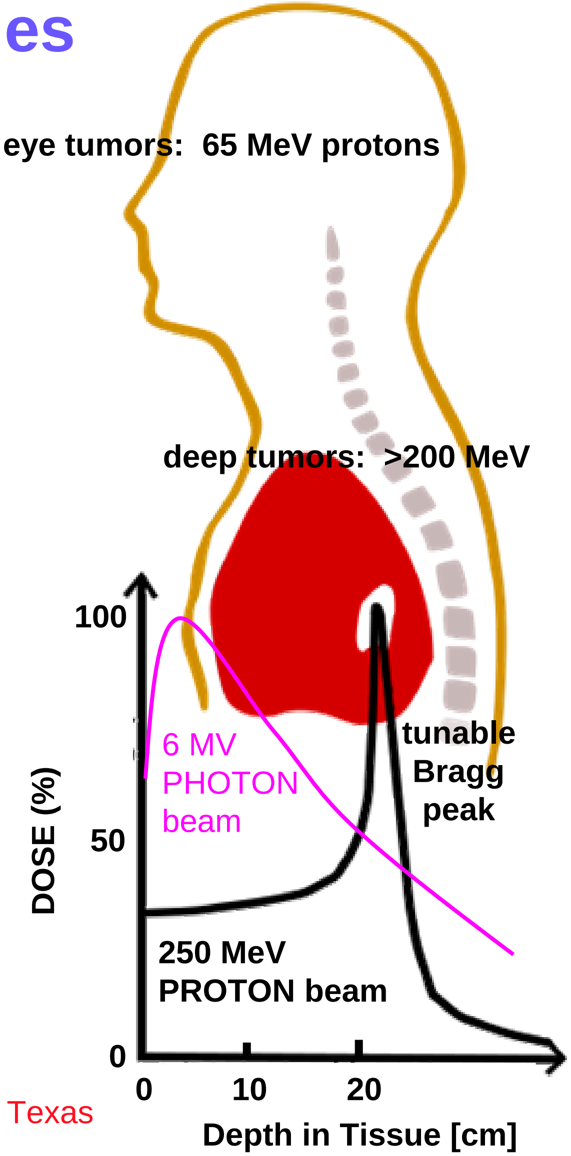

"There are too few physicists in the world, and they are an incredibly important part of doing this... We have one of the largest physics departments in the world, with more than 50 medical physicists."

--- Dr. James D. Cox, head of Radiation Oncology at MD Anderson Cancer Center, Houston, Texas

Laser proton therapy could be much smaller & cheaper:

Fourkal, *Med. Phys.* **29**, 2788 (2002)
Malka, *Med. Phys.* **31**, 1587 (2004)

MeV proton beams create uniform Warm Dense Matter (WDM) for precise Equation-of-State Measurements

Dyer, *Phys. Rev. Lett.* **101**, 015002 (2008)
Patel, *Phys. Rev. Lett.* **91**, 125004 (2003)

Streaked Optical Pyrometry measures sample temperature vs. time

QuickTime™ and a decompressor are needed to see this picture.

QuickTime™ and a decompressor are needed to see this picture.

Chirped-Pulse Interferometry simultaneously measures target expansion into vacuum.

Ultrashort pulses of laser-generated MeV protons provide:

- more uniform volumetric heating over µm scale lengths than fs laser pulses
- isochoric heating to kT ~ 20 eV with higher efficiency than laser-generated hot electrons or x-rays

Dyer, *J. Mod. Opt.* **50**, 2495 (2003)

Results show SESAME Livermore equation-of-state tables to be accurate in a dense plasma regime where few previous experiments were available.

SUMMARY

Intense ultrashort laser pulses heat solid targets isochorically to exotic states

Laser absorption mechanisms ...

- collisional (inverse Bremsstrahlung)
- collisionless (RA, VH, j x B)

... are distinguished by careful pump-probe measurements

Relativistic interactions yield ultrafast secondary radiation...

- MeV hot electrons $\rightarrow$ fast ignition of laser fusion, fs x-rays, proton acceleration
- keV x-rays $\rightarrow$ fs structural dynamics of condensed matter
- MeV protons $\rightarrow$ cancer therapy, rare isotope production, flash radiography,

... and the strongest B fields every measured in a laboratory

- Mgauss magnetic fields $\rightarrow$ physics of white dwarfs & neutron stars